Supporting Information

Self-assemblies of cell-penetrating peptides and ferrocifens: design and biological evaluation of an innovative platform for lung cancer treatment

Léna Guyon[a1], Abdallah Ladaycia[a1], Agnese Bosio[a], Laurent Lemaire[a,b], Florence Franconi[a,b], Bénédicte Lelièvre[c], Nolwenn Lautram[a], Pascal Pigeon[d,e], Gérard Jaouen[d,e], Catherine Passirani[a], Elise Lepeltier[*a,f]

[a] Univ Angers, Inserm, CNRS, MINT, SFR ICAT, F-49000 Angers, France
[b] Univ Angers, Univ Rennes, INRAE, Inserm, CNRS, PRISM, Biogenouest, F-49000 Angers, Rennes, France France
[c] Centre régional de pharmacovigilance, Laboratoire de pharmacologie-toxicologie, CHU Angers, 4 rue Larrey, F-49100 Angers, France
[d] CNRS, Institut Parisien de Chimie Moléculaire (IPCM), Sorbonne Université, 4 Place Jussieu, 75005 Paris, France
[e] PSL, Chimie ParisTech, 11 Rue Pierre et Marie Curie, 75005 Paris, France
[f] Institut Universitaire de France (IUF)

*E-mail: elise.lepeltier@univ-angers.fr
[1] : authors contributed equally to this work

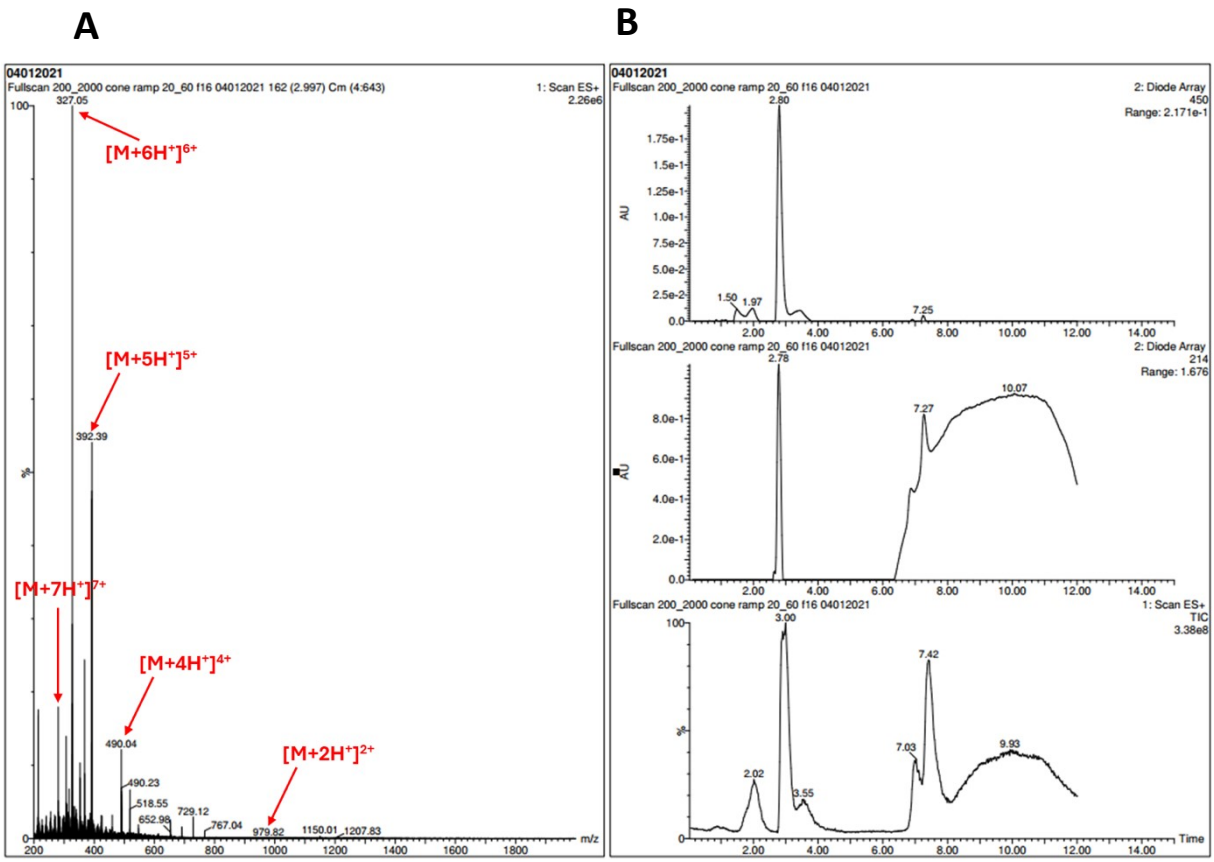

Figure S1. Mass spectroscopy analysis of Arg_9-P819. (A) Mass spectra of the purified Arg_9-P819 showing the different pics corresponding to m/z of the pure molecule. (B) Chromatogram of the pure product detected at 214 nm (middle part) for the peptide part and at 450 nm for the ferrocifen part (top part). At the bottom, the Total Ion Chromatogram (TIC) of the conjugate. The baseline shape on the middle and bottom part of the figure are due the chromatography analysis method: a gradient of water and acetonitrile mixture.

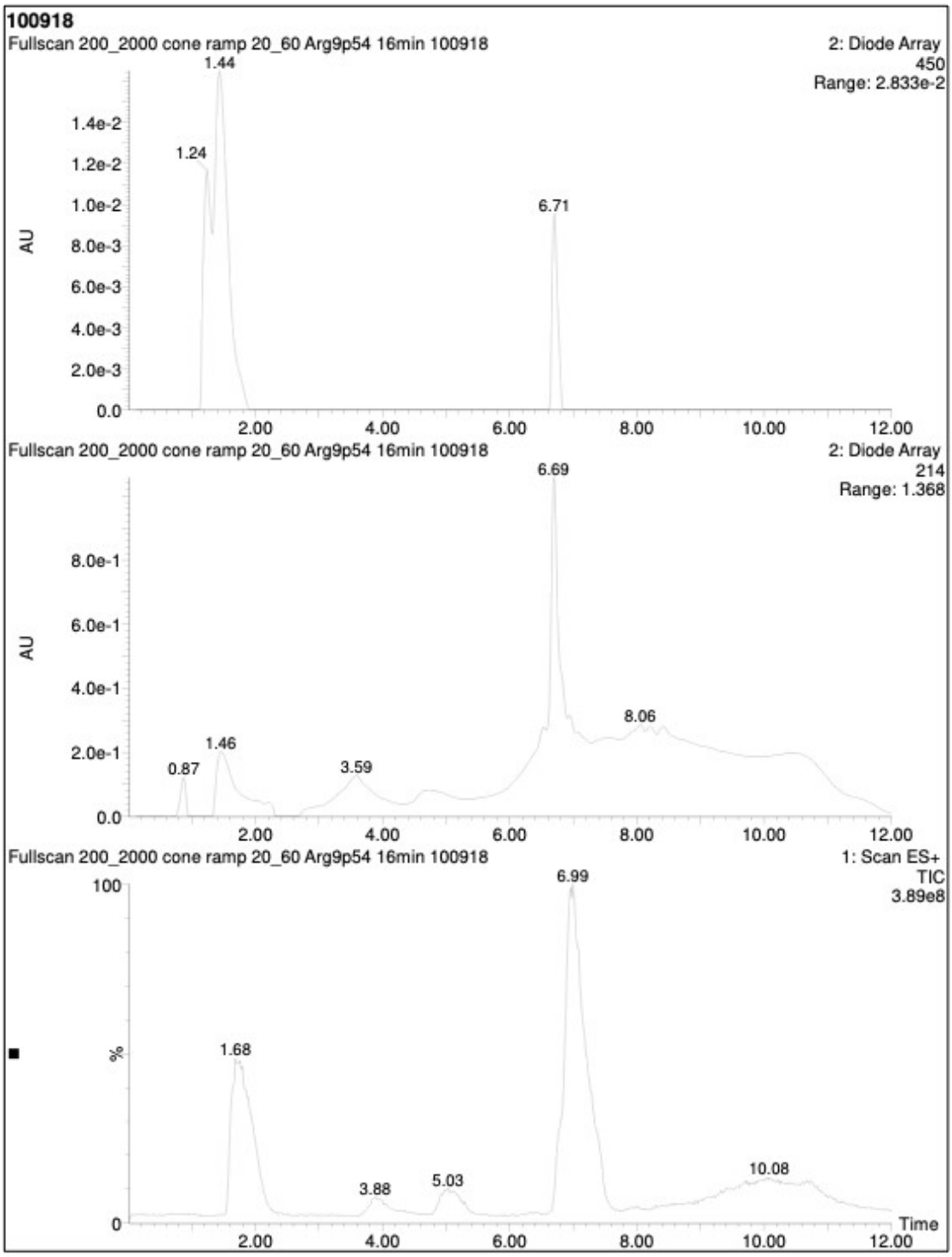

Figure S2. Chromatograms obtained at 214 (middle part) and 450 nm (top part) of the purified conjugate Arg_9-P54: the retention time of the compound is at 6.7 min for the UV detector and at 6.99 min for the MS detector, the last detector being after the UV detector in the channel.

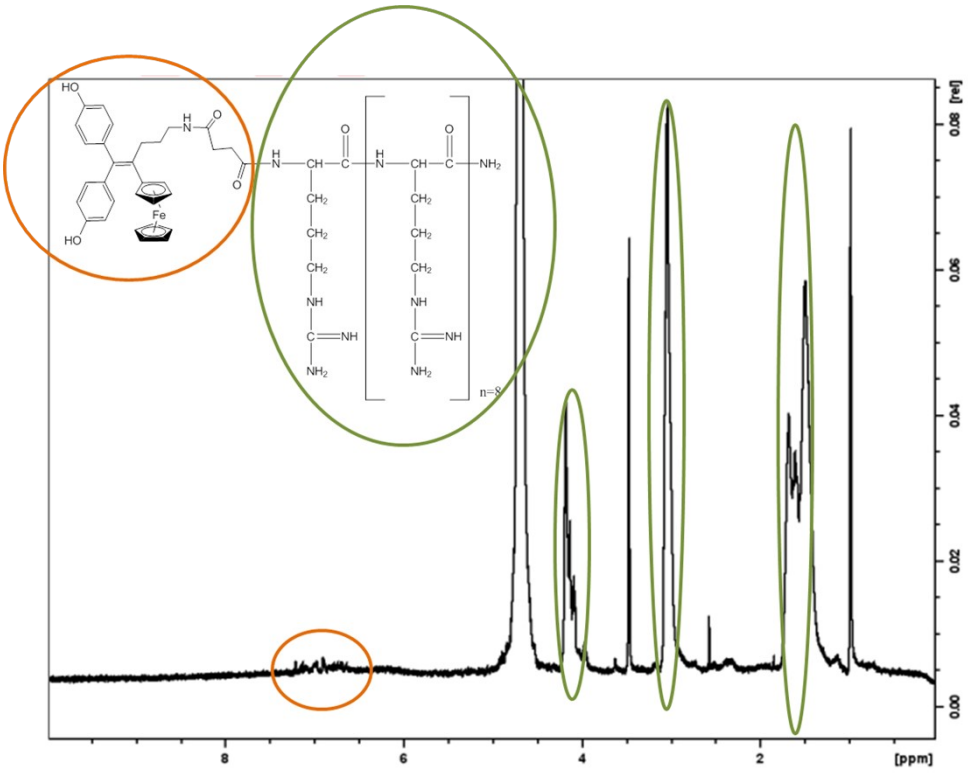

Figure S3. ^{1}H NMR spectrum of Arg_9-P819 in deuterated DMSO.

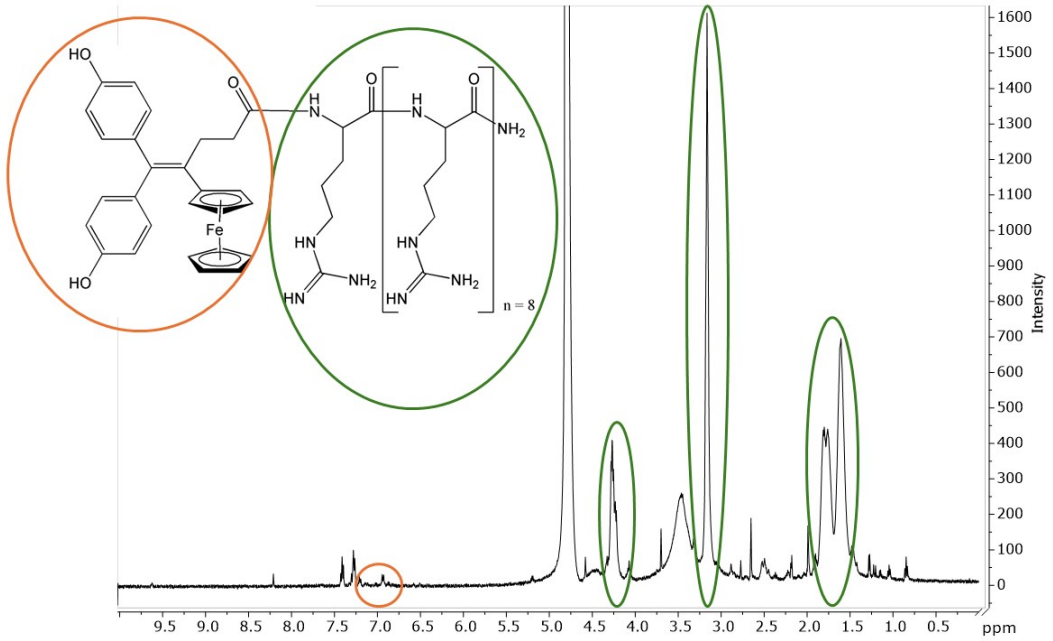

Figure S4. ^{1}H NMR spectrum of Arg_9-P54 in deuterated DMSO.

Supplementary Section S5: ^{1}H NMR analysis of PEG-P54

^{1}H NMR (400 MHz, DMSO-d6) : δ 2.30 (t, 2 H, CH_2 of P54), 2.73 (t, 2 H, CH_2 of P54), 3.51 (s, 185H, CH_2 of PEG), 3.83 (t, 2H, C_5H_4 of P54), 4.09 (t, 2H, C_5H_4 of P54), 4.12 (s, 5H, Cp of P54), 6.61 (d, 2H, C_6H_4 of P54), 6.71 (d, 2H, C_6H_4 of P54), 6.77 (d, 2H, C_6H_4 of P54), 6.97 (d, 2H, C_6H_4 of P54), 9.28 (s, 1H, OH), 9.34 (s, 1H, OH), 12.01 (s broad, 1H, OH).

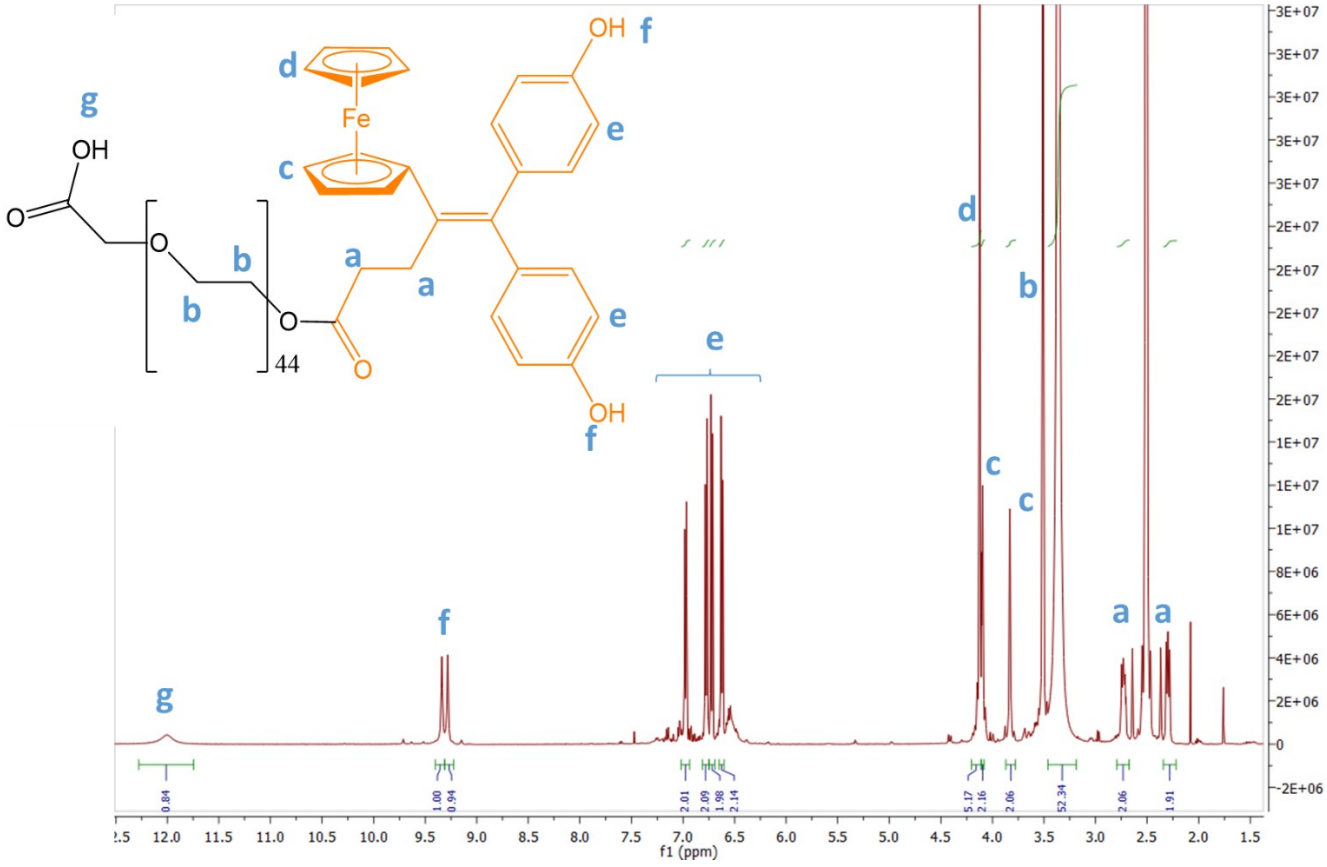

Figure S5. ^{1}H NMR spectrum of PEG-P54 in deuterated DMSO.

Supplementary Section S6: ^{1}H NMR and ^{13}C NMR analysis of PEG-P819

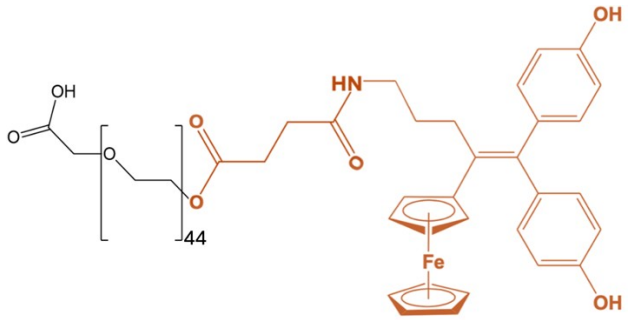

^{1}H NMR (DMSO-d_6): δ 1.48-1.59 (m, 2H, CH_2 P819), 2.28 (t, *J* = 7.1 Hz 2H, CH_2 P819), 2.42 (t, *J* = 7.1 Hz, 2H, CH_2 P819), 2.43-2.50 (m, 2H, CH_2-C=C P819), 2.85 (d, *J* = 7.1 Hz, 2H, CH_2N P819), 3.5 (s, CH_2 of PEG), 4.06 (t, *J* = 2.0 Hz, 2H, C_5H_4), 4.09 (t, *J* = 2.0 Hz, 2H, C_5H_4), 4.10 (s, 5H, Cp), 6.62 (d, *J* = 8.5 Hz, 2H, C_6H_4), 6.71 (d, *J* = 8.5 Hz, 2H, C_6H_4), 6.77 (d, *J* = 8.5 Hz, 2H, C_6H_4), 6.94 (d, *J* = 8.5 Hz, 2H, C_6H_4), 7.79 (q, *J* = 6.0 Hz, 1H, NH).

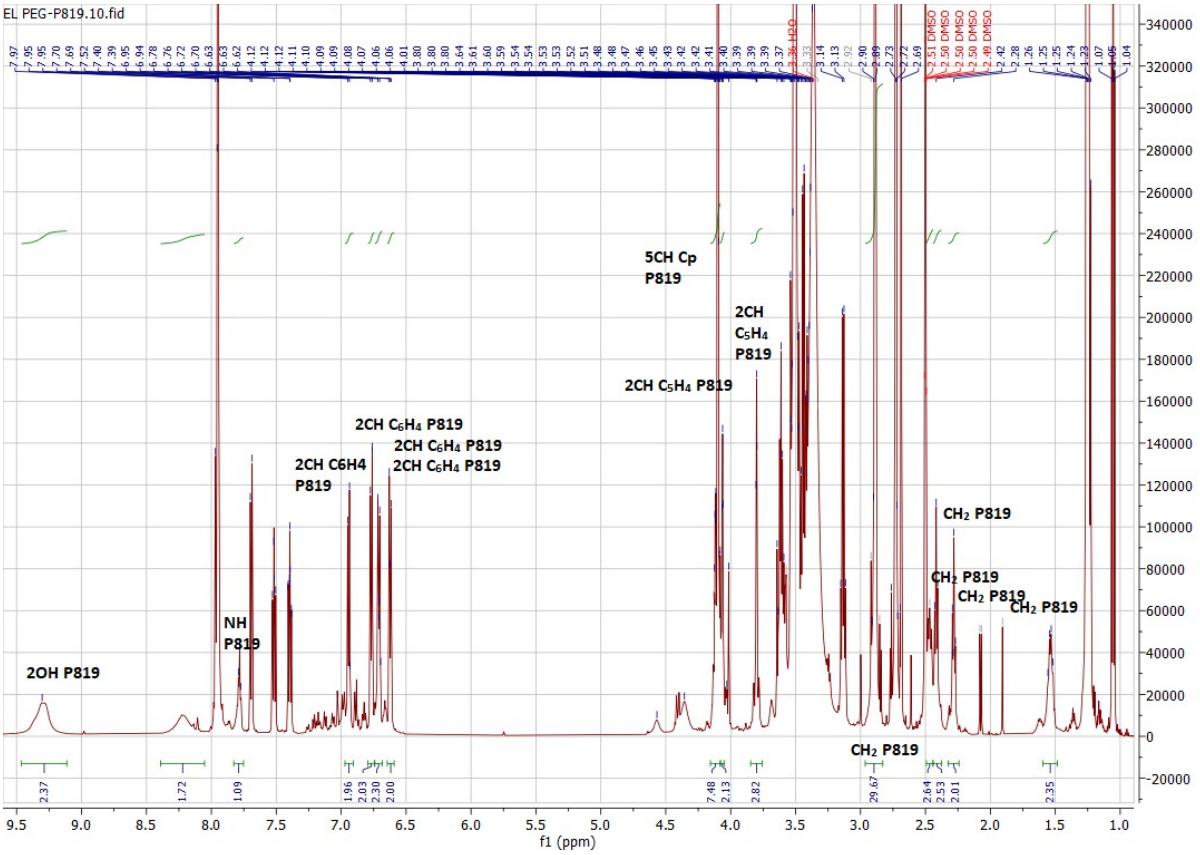

^{13}C NMR (DMSO-d_6): δ 29.7 (CH_2 P819), 30.5 (CH_2 P819), 30.9 (CH_2 P819), 32.2 (CH_2 P819), 39.2 (CH_2 P819), 69.2 (2CH C_5H_4), 69.46 (5CH Cp), 69.53 (2CH C_5H_4), 70.0 (2CH_2 of PEG), 87.1 (C C_5H_4), 115.5 (2x2CH C_6H_4), 130.4 (2CH C_6H_4), 130.8 (2CH C_6H_4), 133.7 (C), 135.7 (C), 136.1 (C), 138.5 (C), 156.0 (C-OH), 156.1 (C-OH), 171.1 (CO P819), 174.3 (CO P819), 177.9 (COO of the PEG-P819).

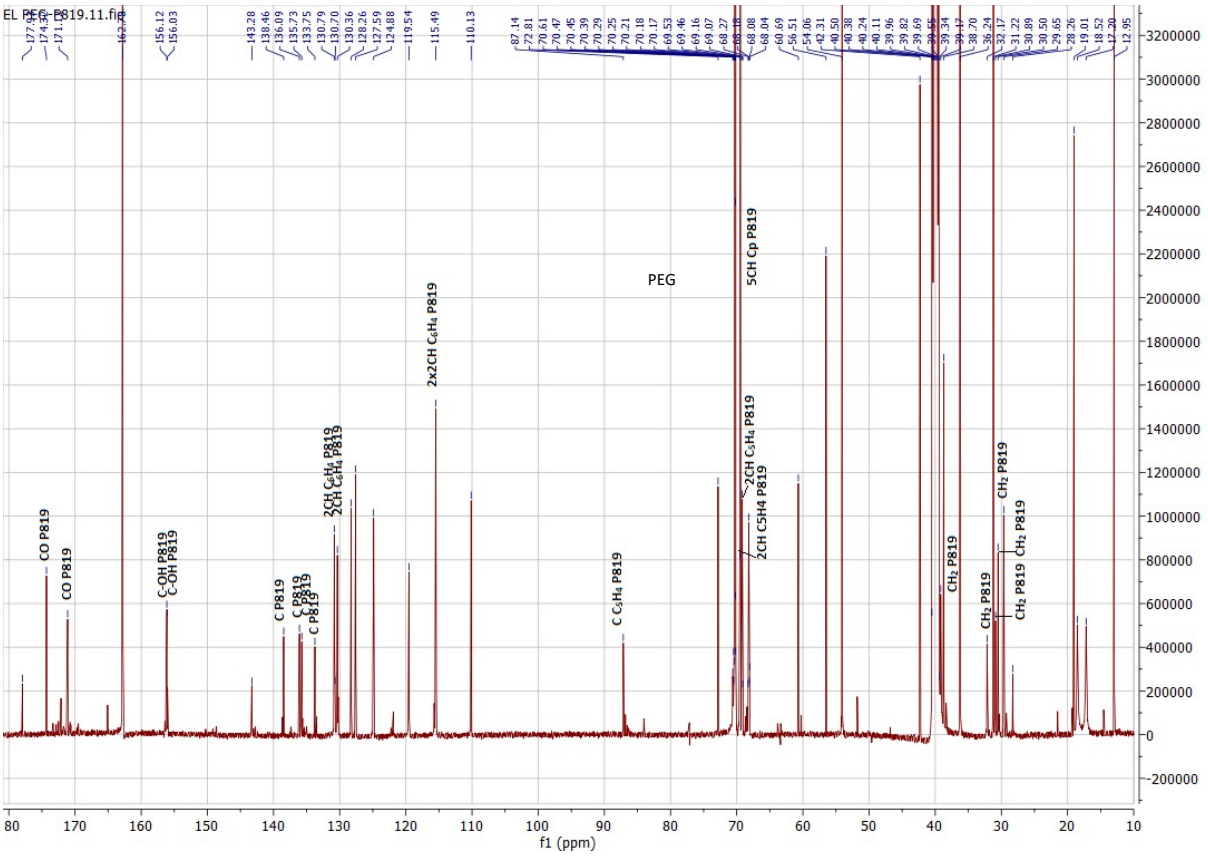

Figure S6. ^{1}H NMR spectrum of PEG-P819 on the top and ^{13}C NMR spectrum of PEG-P819 in DMSO-d6 bellow.

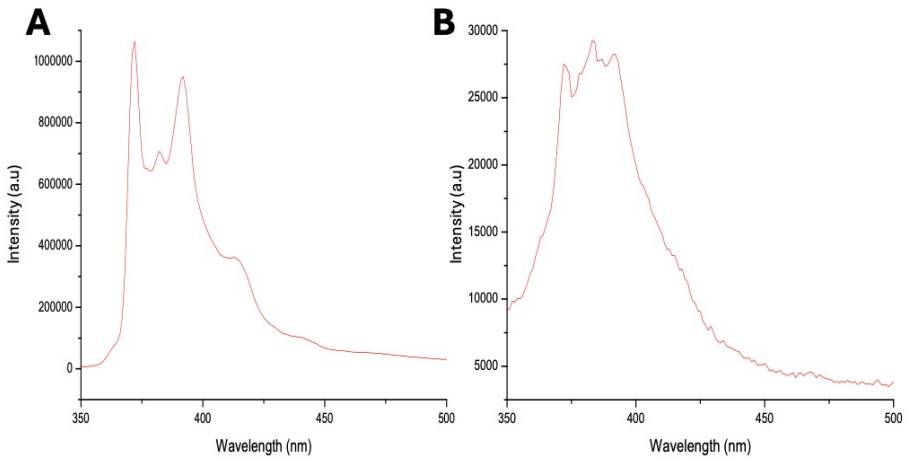
A
Intensity (a.u)
1000000
800000
600000
400000
200000
0
350
400
450
500
Wavelength (nm)

B
Intensity (a.u)
30000
25000
20000
15000
10000
5000
350
400
450
500
Wavelength (nm)

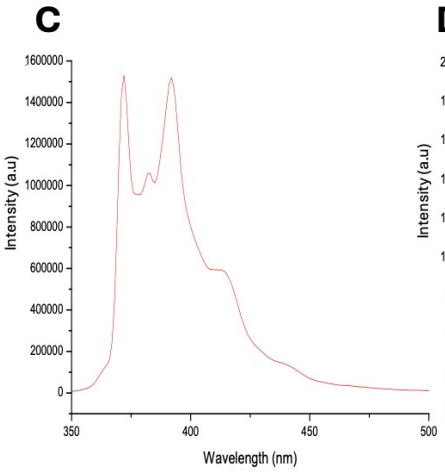
C
Intensity (a.u)
1600000
1400000
1200000
1000000
800000
600000
400000
200000
0
350
400
450
500
Wavelength (nm)

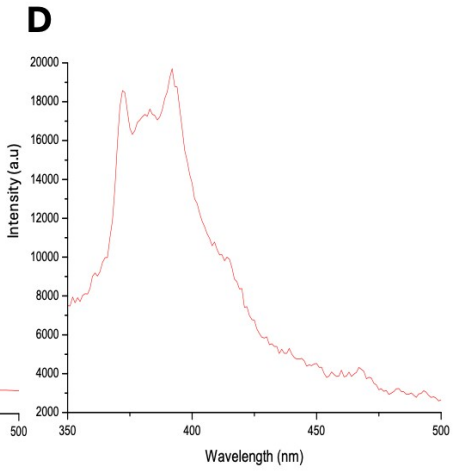
D
Intensity (a.u)
20000
18000
16000
14000
12000
10000
8000
6000
4000
2000
350
400
450
500
Wavelength (nm)

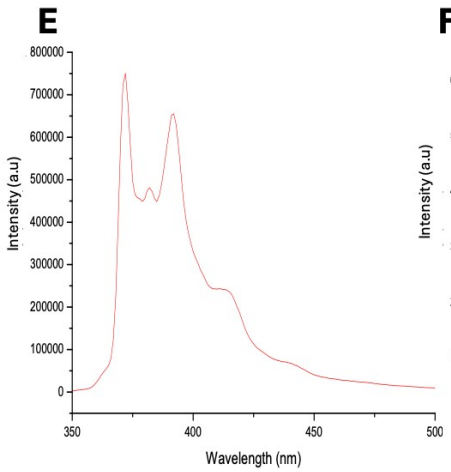
E
Intensity (a.u)
800000
700000
600000
500000
400000
300000
200000
100000
0
350
400
450
500
Wavelength (nm)

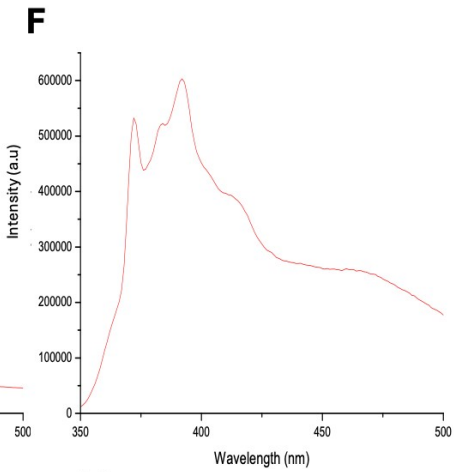
F
Intensity (a.u)
600000
500000
400000
300000
200000
100000
0
350
400
450
500
Wavelength (nm)

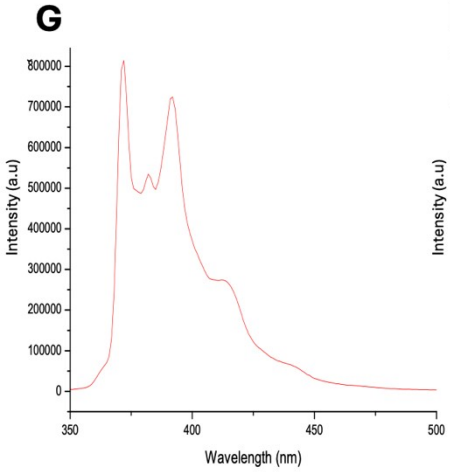
G
Intensity (a.u)
800000
700000
600000
500000
400000
300000
200000
100000
0
350
400
450
500
Wavelength (nm)

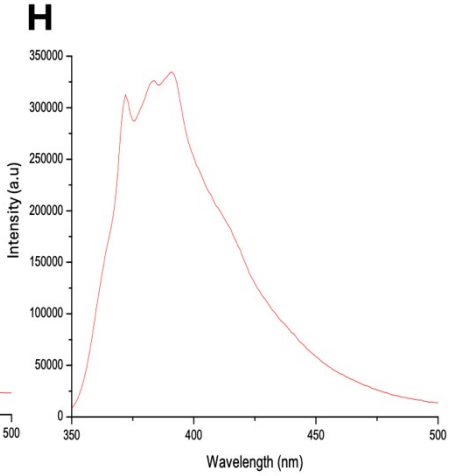
H
Intensity (a.u)
350000
300000
250000
200000
150000
100000
50000
0
350
400
450
500
Wavelength (nm)

Figure S7. Using the pyrene method, representative fluorescent spectra for calculating the CAC: P54 at 10 μM (A) and at 3.2 mM (B), PEG-P54 at 50 μM (C) and at 600 μM (D), Arg_9-P54 at 6 μM (E) and at 1 mM (F) and Arg_9-P819 at 1 μM (G) and at 1.8 mM (H).

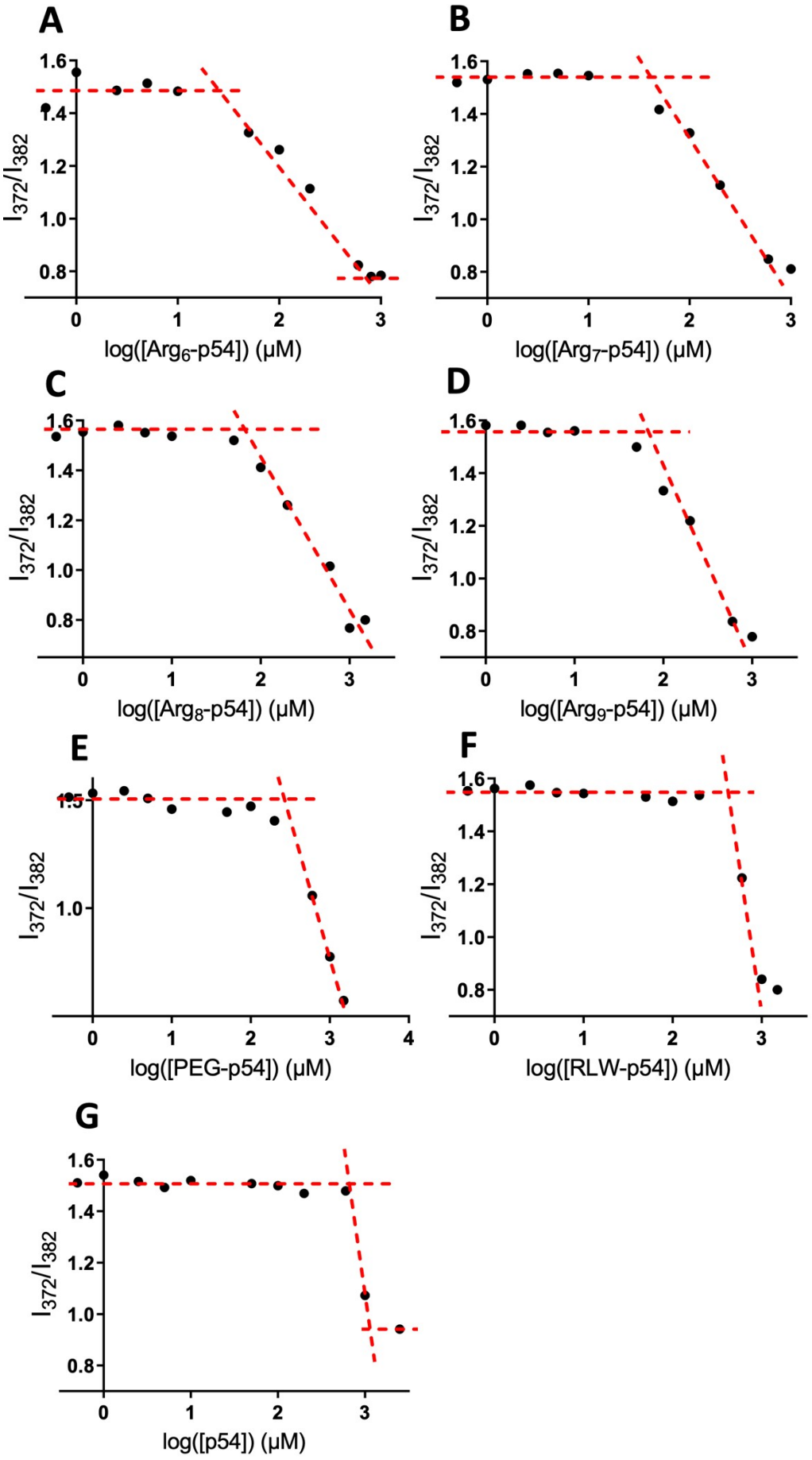
A
B
C
D
E
F
G
I_{372}/I_{382}
log([Arg6-p54]) (μM)
log([Arg7-p54]) (μM)
log([Arg8-p54]) (μM)
log([Arg9-p54]) (μM)
log([PEG-p54]) (μM)
log([RLW-p54]) (μM)
log([p54]) (μM)

Figure S8. Quotient of vibrational band intensities (I_1/I_3) as a function of log [Arg_6-P54] (A), log [Arg_7-P54] (B), log [Arg_8-P54] (C), log [Arg_9-P54] (D), log [PEG-p54] (E), log [RLW-P54] (F) and [P54] (G).

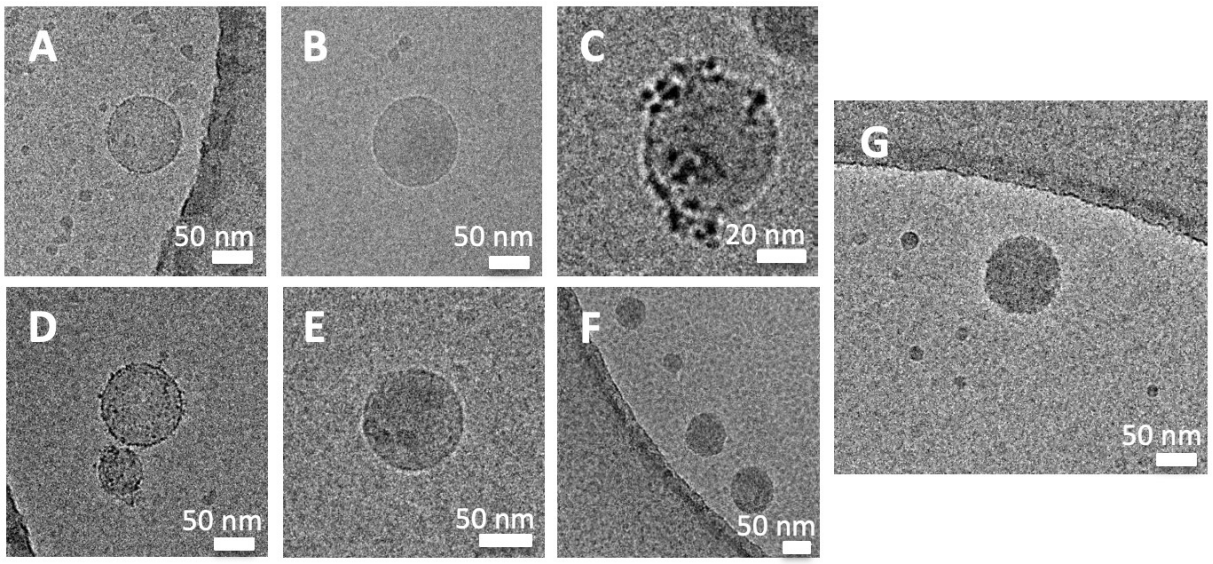

Figure S9. Representative Cryo-TEM images of self-assemblies formed from Arg_6-P54 (A)[1], Arg_7-P54 (B)[1], Arg_8-P54 (C)[1], Arg_9-P54 (D)[1], RLW-P54 (E)[1], PEG-P54 (F) and Arg_9-P54/PEG-P54 (G).

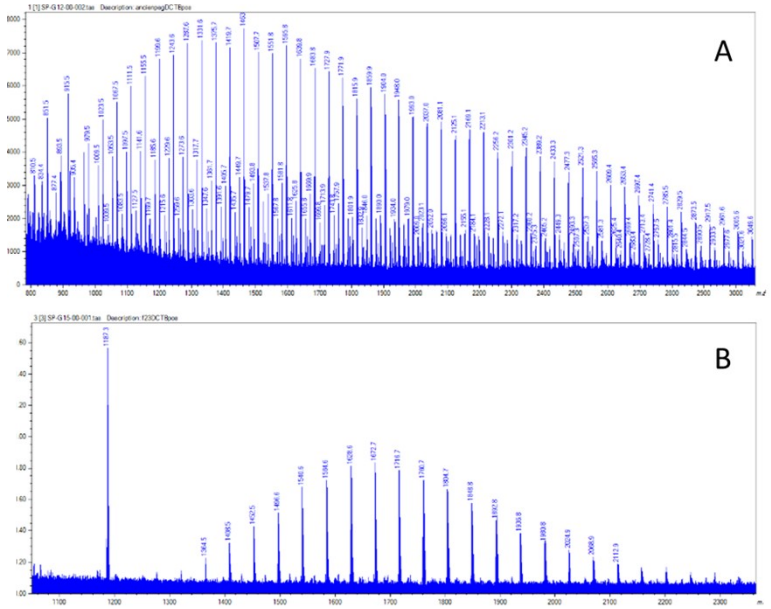

Figure S10. MALDI spectrum of free PEG (A), and of PEG-P819 (B), where a switch of the mass spectrum is observed and corresponds to the addition of P819 (M_{P819} = 569.47 g.mol^{-1}).

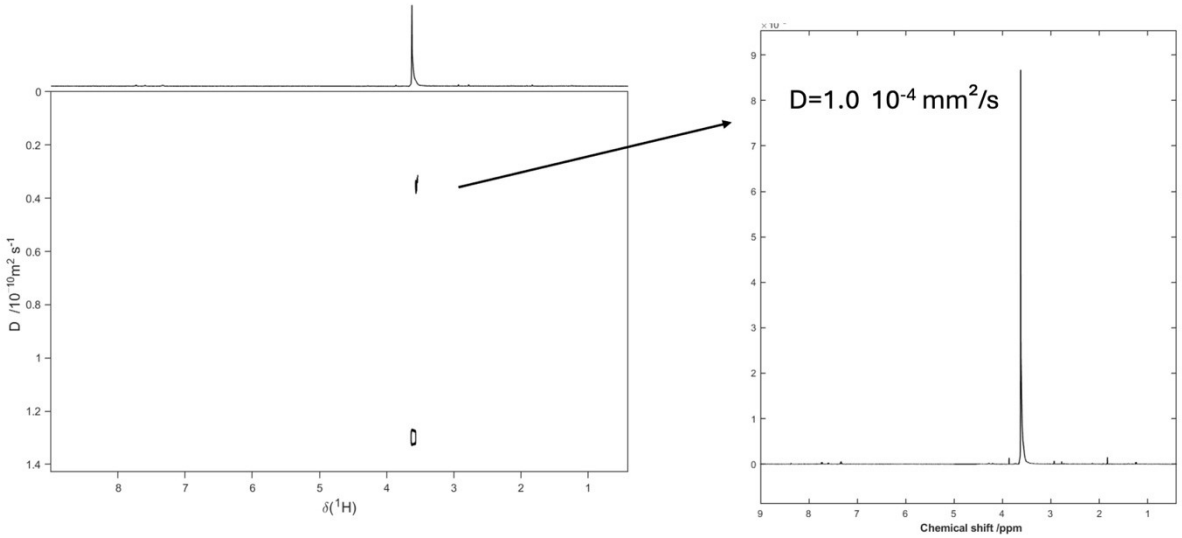

Figure S11. DOSY ^{1}H spectrum (left) of PEG-P54 suspension in deuterated water at 25 °C after filtration through 0.2 µm and corresponding to one main component SCORE analysis (right).

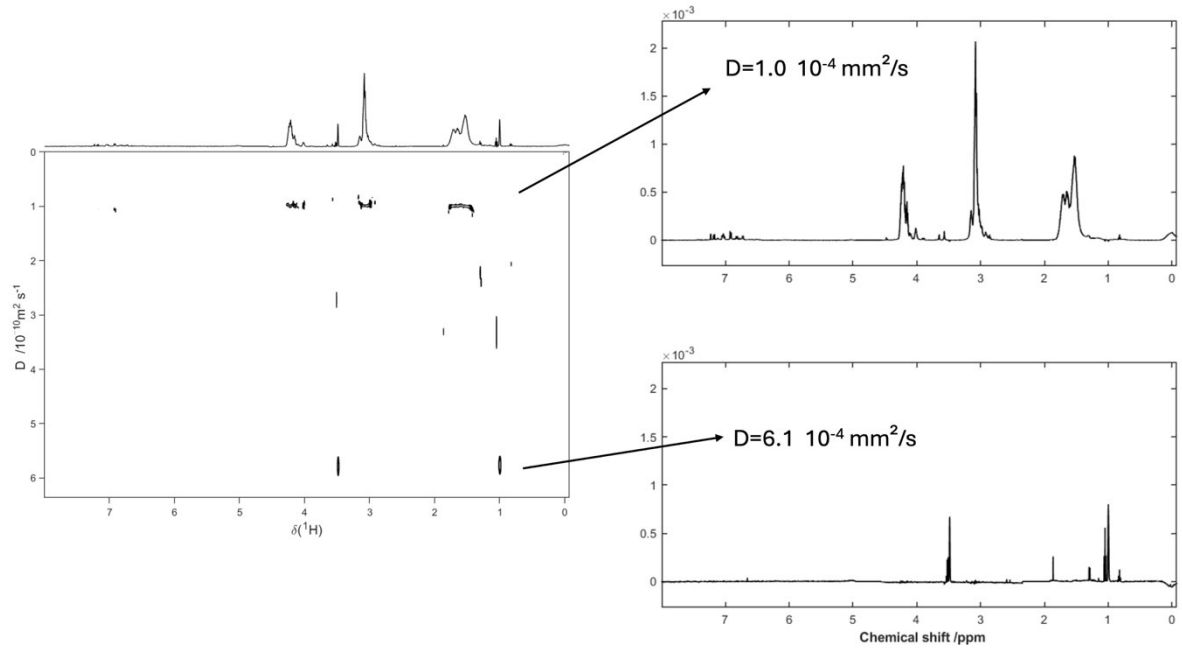

Figure S12. DOSY ^{1}H spectrum (left) of Arg_9-P819/PEG-P819 suspension in deuterated water at 25 °C after filtration through 0.2 µm and corresponding two components SCORE analysis (right).

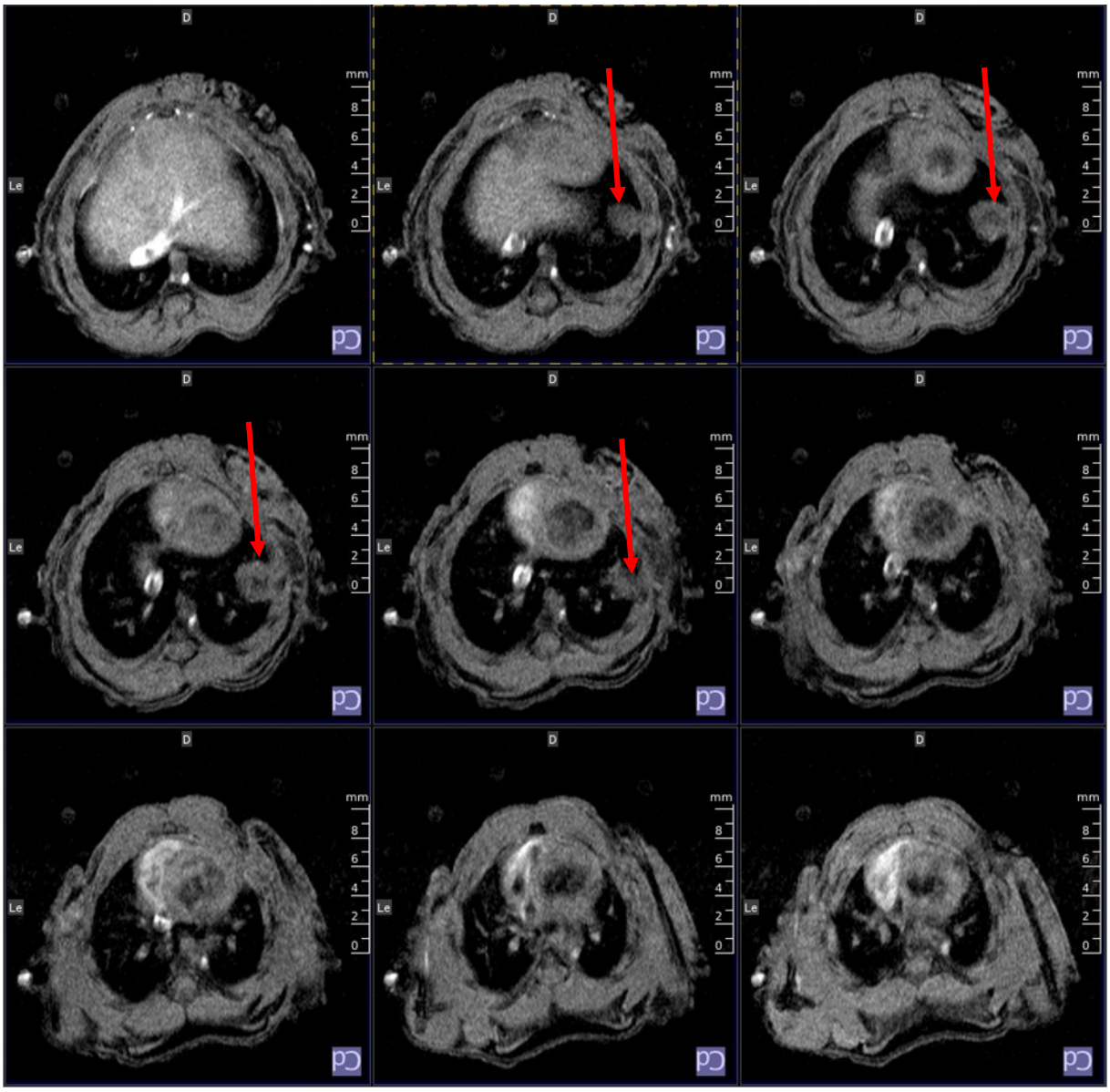

Figure S13. intrapulmonary tumor detected by MRI (the red arrow). This representative picture shows 9 slices of 0.75 millimeters of thickness per slide. Starting from the upper left image to the lower right ones, the slices were taking from the lower part to the upper part of the mouse.

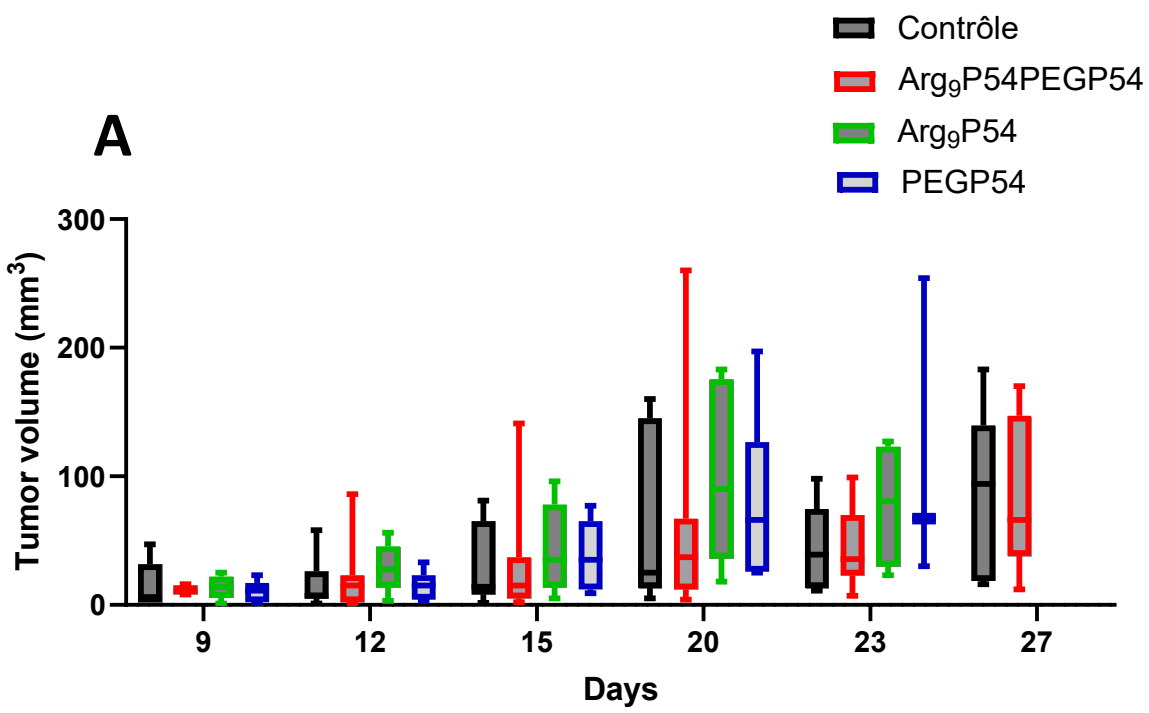
A
Contrôle
Arg9P54PEGP54
Arg9P54
PEGP54
Tumor volume (mm3)
300
200
100
0
9
12
15
20
23
27
Days

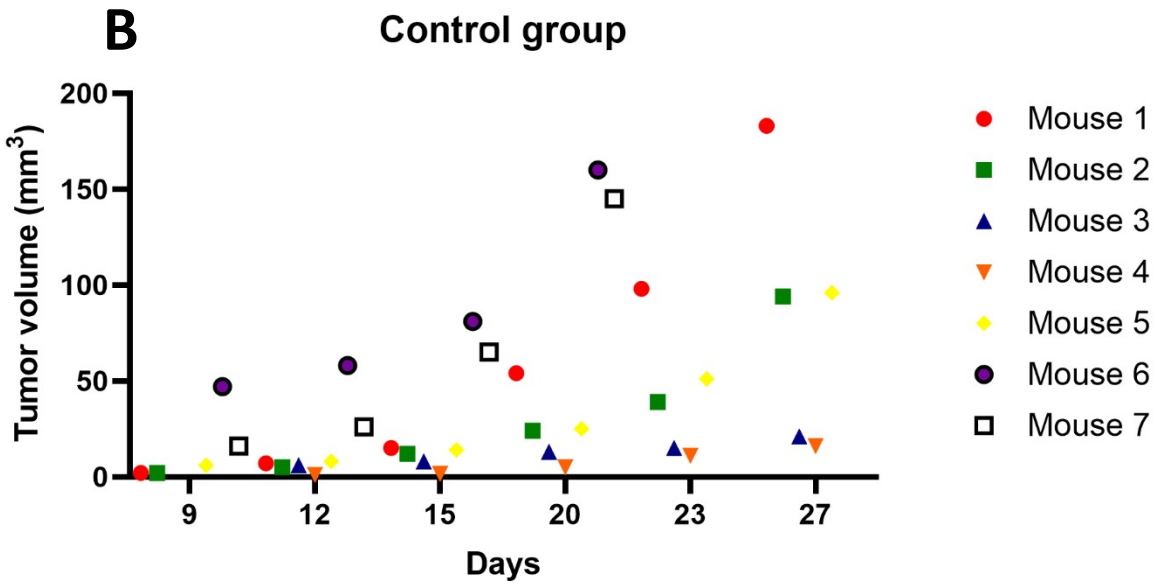
B
Control group
Tumor volume (mm3)
200
150
100
50
0
9
12
15
20
23
27
Days
Mouse 1
Mouse 2
Mouse 3
Mouse 4
Mouse 5
Mouse 6
Mouse 7

C

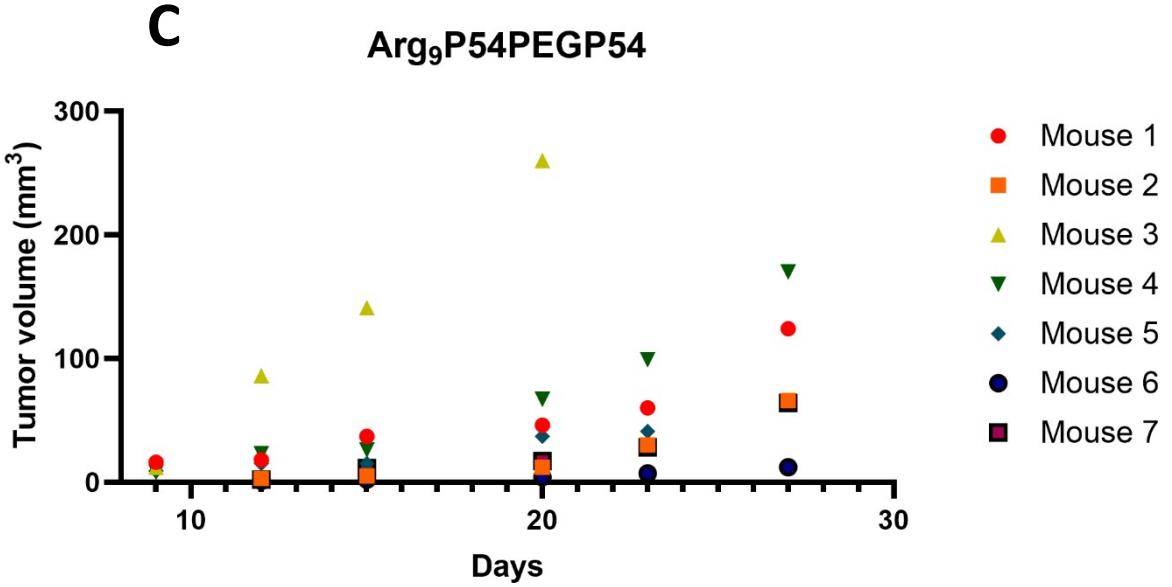
Arg9P54PEGP54
Tumor volume (mm3)
300
200
100
0
10
20
30
Days
Mouse 1
Mouse 2
Mouse 3
Mouse 4
Mouse 5
Mouse 6
Mouse 7

D

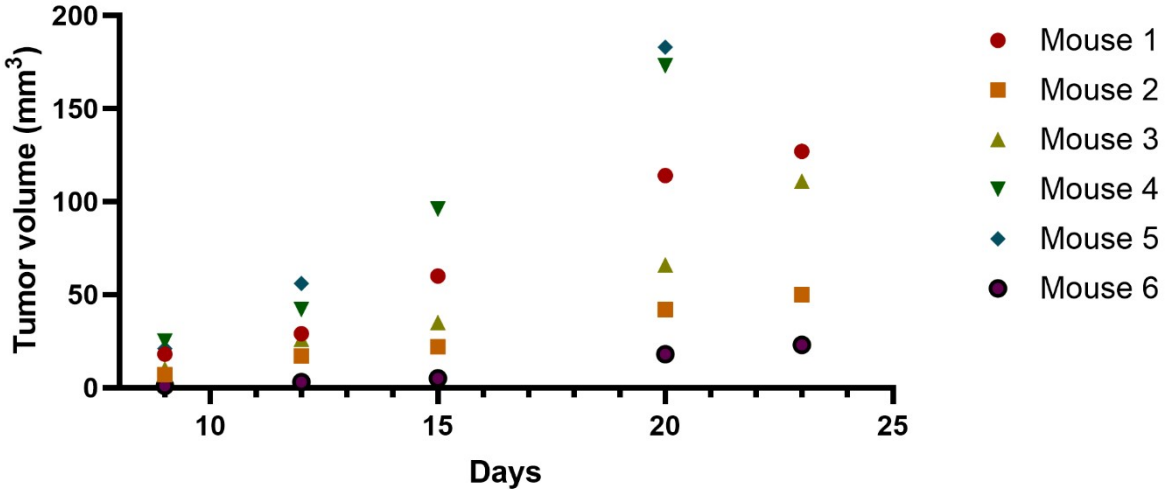
Arg9P54
Tumor volume (mm3)
200
150
100
50
0
10
15
20
25
Days
Mouse 1
Mouse 2
Mouse 3
Mouse 4
Mouse 5
Mouse 6

E

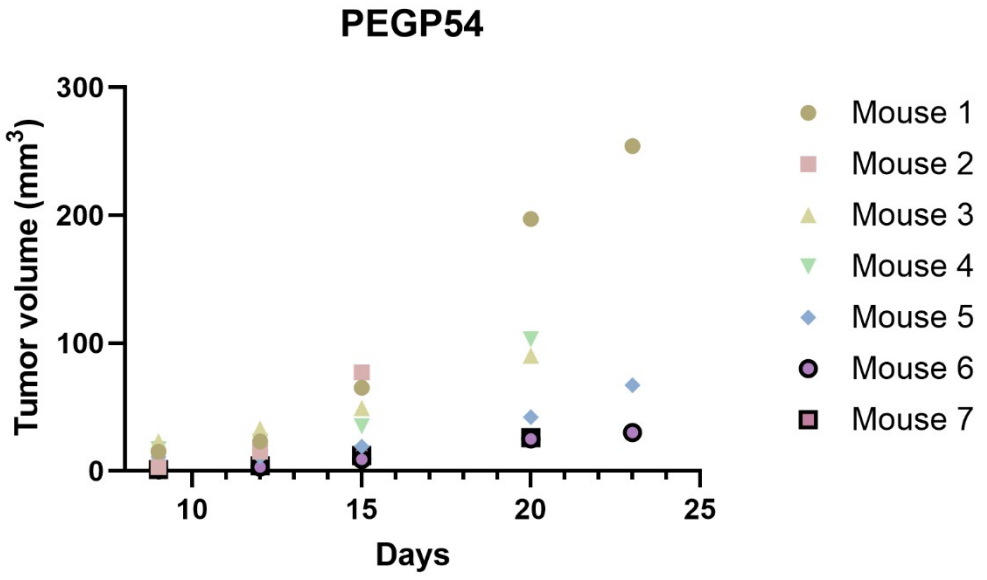
PEGP54
Tumor volume (mm3)
300
200
100
0
10
15
20
25
Days
Mouse 1
Mouse 2
Mouse 3
Mouse 4
Mouse 5
Mouse 6
Mouse 7

Figure S14. Global tumor size evolution for 27 days (A) and the detailed description per group of study: Control group (B), Arg_9-P54/PEG-P54 (C), Arg_9-P54 (D) and PEG-P54 (E).

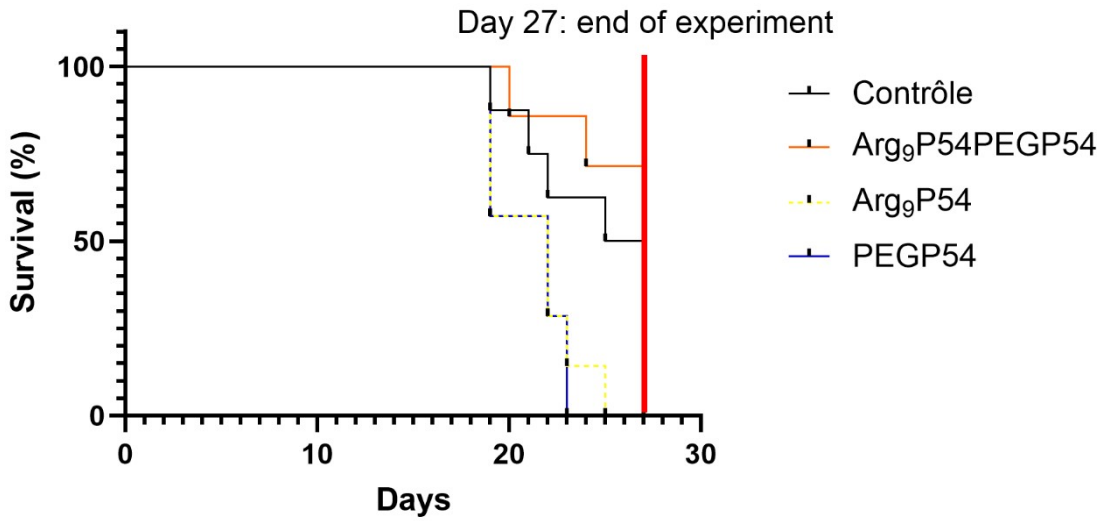

Figure S15. Mice survival during the course of the study, 27 days.

References

1. Guyon, L. *et al.* Importance of Combining Advanced Particle Size Analysis Techniques To Characterize Cell-Penetrating Peptide–Ferrocifen Self-Assemblies. *J. Phys. Chem. Lett.* **10**, 6613–6620 (2019).